東北医科薬科大学

審査学位論文（博士）

氏名（本籍）	リュウ　　ケンウェイ 劉　　健　偉　（中国）
学位の種類	博士（薬科学）
学位記番号	博薬学第 27 号
学位授与の日付	令和 6 年 3 月 8 日
学位授与の要件	学位規則第 4 条 1 項該当
学位論文題名	Deubiquitinase BRCC36 associates with FLT3-ITD to regulate its protein stability and intracellular signaling in acute myeloid leukemia （脱ユビキチン化酵素 BRCC36 は急性骨髄性白血病において FLT3-ITD との結合でタンパク質の安全性と細胞内シグナル伝達を制御する）
論文審査委員	主査　　教 授　山口　芳樹
	副査　　教 授　藤村　　務
	副査　　教 授　顧　　建国

Deubiquitinase BRCC36 associates with FLT3-ITD to regulate its protein stability and intracellular signaling in acute myeloid leukemia

令和 6 年 3 月

東北医科薬科大学大学院薬学研究科

劉健偉

Contents

1. Introduction

Intracellular protein homeostasis is regulated by protein synthesis and degradation (1). Proteins are degraded by two main proteolytic systems: the autophagy-lysosome pathway and the ubiquitin-proteasome system (2). Ubiquitination mediates the targeting of a substrate to the proteasome and the lysosome, a significant site for protein degradation (3). Ubiquitination, a process that forms a bond between ubiquitin and the lysine residue at the target site of a protein, is one of the multifaceted post-translational modifications regulating almost all of the cellular processes (4). This process, both dynamic and reversible, is regulated by ubiquitin ligases and deubiquitinases (DUBs) (5). Previous studies have demonstrated a variety of linkages within ubiquitin chains, determined by the ubiquitination sites (6). Among them, K48- and K63-linked polyubiquitin chains are the most well-studied members and the most abundant types in cells (7). The role of K48-linked chains is to target substrates to the proteasome for degradation (8). In contrast, the K63 chain performs various functions, including DNA damage repair, kinase signaling pathways, receptor trafficking, and ribosomal biogenesis (9). BRCA1/BRCA2-containing complex subunit 36 (BRCC36), a specific K63 DUB, comprises a functional metalloprotease domain and a predicted coiled-coil region (10), and belongs to the JAMM/MPN+ family of deubiquitinating enzymes. BRCC36 requires the formation of multi-subunit complexes to express its isopeptidase activity. In the nucleus, BRCC36 and the subunits MERIT40, BRCC45/BRE, Abraxas, and RAP80 form the BRCA1-A complex to participate in DNA damage repair (11). In the cytoplasm, BRCC36, together with the subunits MERIT40/NBA1, BRCC45/BRE, and Abro1/KIAA0157, forms a BRISC (BRCC36 isopeptidase complex) complex to play significant roles in various signaling pathways (12).

Acute myeloid leukemia (AML) is adults' most common form of acute leukemia. It represents the deadliest type of this disease (13). Fms-like tyrosine kinase 3 (FLT3) is one of the most frequently mutated genes in AML (14). As a cell-surface receptor for the cytokine FLT3 ligand (FL), FLT3 can regulate the differentiation, proliferation, and survival of hematopoietic progenitor cells (15). Internal tandem duplication (ITD) of

the juxtamembrane domain of FLT3 is the primary kinase mutation in human AML, and the other predominant point mutation is the tyrosine kinase domain (TKD) mutation (16), as shown in Figure 1. AML patients harboring mutations are known to have lower survival rates and higher relapse rates, underscoring the urgent need for research into novel strategies to target mutant FLT3 (17). A previous study comparing ITD and TKD mutations found that ITD was associated with worse relapse-free survival, an association not found with TKD mutations (18,19). The majority of patients harboring ITD experience relapse within a short period after discontinuation of chemotherapy (20). The development of tyrosine kinase inhibitors (TKIs) blocking ITD became a rational therapeutic concept (21).

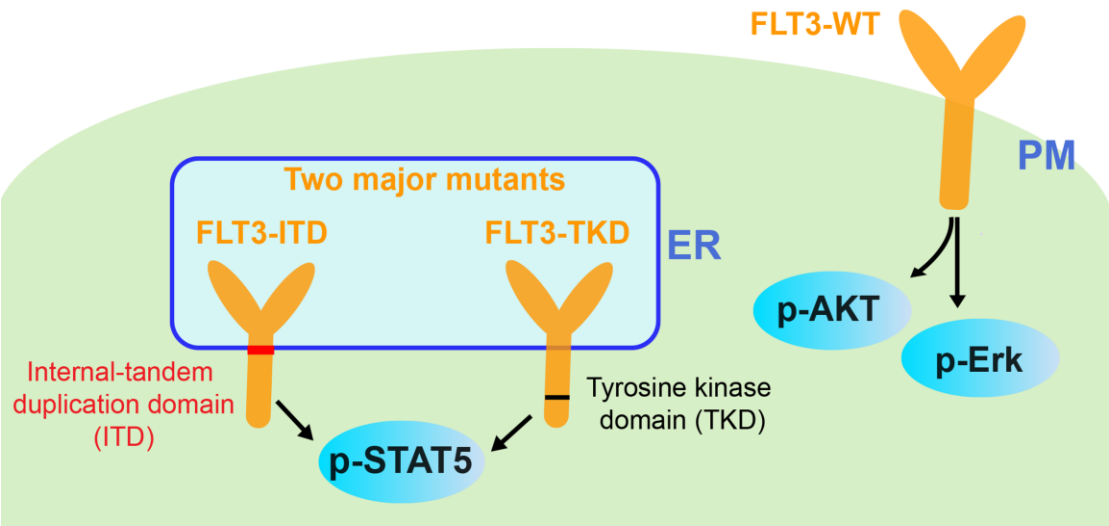

Figure 1. Localization and cellular signaling of FLT3-WT and mutants.

Thus far, several experiments have revealed exclusive interactions between ITD or TKD and other molecules. FLT3-ITD, but not TKD, uses Src to activate STAT5 (22). The association of NPM1c with FLT3-TKD shifts the TKD localization and activates STAT5 signaling (23). ITD and TKD have different abilities to induce the activation of signaling pathways (24,25), which underscores the importance of distinguishing these mutants in disease progression and treatment.

Exploring the protein interactome is a common approach to uncovering new properties of target proteins. Mass spectrometry with affinity purification is a frequently used strategy to identify novel protein interactions. Proximity labeling is performed by ligases that catalyze the transition of an inert small molecular substance into a highly

reactive form and connect proximal endogenous proteins (26). TurboID uses biotin and ATP to generate biotin-5′-AMP. This reactive intermediate can rapidly label lysine residues of the near proteins. TurboID has higher activity than previously described biotin proximity labeling methods, such as BioID, enabling higher temporal resolution and broader application in vivo (26).

In the present study, we used proximity labeling technology combined with the LC-MS analysis to distinguish the properties of FLT3 mutants. We found that FLT3-ITD is specifically associated with BRCC36, which hydrolyzes K63-linked polyubiquitin chains of ITD. The association with BRCC36 specifically enhanced the ITD stability and its mediated intracellular signaling. Conversely, the knockdown of BRCC36 or its inhibitor downregulated ITD expression and downstream signaling. Thus, BRCC36 may be a promising target for novel therapies against FLT3-ITD-positive AML.

2. Materials and methods

2.1 Cell line and cell culture

Parental Ba/F3 cells were cultured in 1640 RPMI with 10% fetal bovine serum (FBS, Gibco), 1 ng/mL recombinant murine interleukin-3 (IL-3) (PeproTech, London, United Kingdom), and 50 μmol/L 2-mercaptoethanol (2-ME) (27). The stably transfected Ba/F3-FLT3-WT cell line was cultured in RPMI with 10% FBS, 1 ng/mL murine IL-3, 400 μg/mL G418, and 50 μmol/L 2-ME. Ba/F3-FLT3-ITD and Ba/F3-FLT3-TKD cells were maintained in RPMI containing 10% FBS with 400 μg/mL G418 and 50 μmol/L 2-ME (28). The human leukemia cell lines MV4-11 and RS4-11 cells were cultured in RPMI medium containing 10% FBS at 37°C and 5% CO_2. The 293T and HeLa cells were cultured in a DMEM medium containing 10% FBS at 37°C and 5% CO_2.

2.2 Antibodies and reagents

FLT3 (3462S), p-STAT5 (4322S), p-Erk1/2 (4370), p-Akt (4060), and peroxidase-conjugated secondary antibody against rabbit (7074S) were purchased from Cell Signaling Technology (Danvers, MA, USA); STAT5 (13-3600) and Lipofectamine 2000 reagent (100014469) were from Thermo Fisher (Waltham, MA, USA); monoclonal antibody against α-tubulin and anti-HA antibody (11867423001) were acquired from Sigma (St. Louis, MO, USA); Peroxidase-conjugated secondary antibody against mouse (AP124P) were from Millipore; anti-BRCC36 antibody (4331) were from ProSci Inc (Poway, CA, USA); mouse antibodies against GM130 (610823) and calnexin (610524) were from BD (NJ, USA). Goat anti-mouse and -rabbit IgG Alexa Fluor 568/488 were purchased from Invitrogen (Carlsbad, CA, USA). Biotin (SKG4828), cycloheximide (CHX, 037-20991), MG132 (139-18451), and thiolutin (T2834) were purchased from Wako (Tokyo, Japan). Quizartinib (AC220, CS-0211) was from Funakoshi (Tokyo, Japan).

2.3 Expression plasmids and transfection

We used the Gateway™ cloning system (Invitrogen) for all overexpression experiments. The 3×HA-TurboID plasmid (107171) (29) was purchased from Addgene.

The cDNA sequences for FLT3-WT, FLT3-ITD, and FLT3-TKD were cloned from the vectors as previously described (27) and inserted into TurboID pENTR/D-TOPO vectors at the N terminus by the in-fusion technology (Takara Bio Inc.). The cDNA sequences of BRCC36 were cloned from 293T cells and inserted into pENTR/D-TOPO vectors containing 2×VSV-tag (30). After confirmed by DNA sequencing, all of the entry vectors were transferred into the pcDNA3.1 vector by LR clonase (Invitrogen) for transient expression. The pRK5-HA-ubiquitin-K63 (17606) (31) plasmid was purchased from Addgene. The FLT3-ITD-K609R plasmid was synthesized by specific primers (Table 1) and sequenced.

Table 1. Primer sequences for plasmids

Names	Sequence (5'-3')
FLT3-F	TACAAAAAAGCAGGCTCCGCGGCCGCACCATGCCGGCGTTGGCG
FLT3-R	TCCACCTCCGCCGCTGCCCACCGAATCTTCGACCTGAGCCTGCG
TurboID-vector-F	GCTGTACAAGTGAAAGGGTGGGCGCGCC
TurboID-vector-R	TGCTCACCATCGATCCACCGCCTCCGCTAC
BRCC36-F	ATGGCGGTGCAGGTGGTGCA
BRCC36-R	TTATTCTAGAGAAGAAAGTTCTTGCATAAGCTCTTCCTTTTCTTGTTGT
VSV-vector-F	AACTTTCTTCTCTAGAATAATGAGCGGCCGCGACTCTA
VSV-vector-R	TGCACCACCTGCACCGCCATAGCGTAATCAGGAACGTCGTACATG
FLT3-ITD-K609R-F	TGATCTCAGATGGGAGTTTCCAAGAGAAAATTT
FLT3-ITD-K609R-R	AACTCCCATCTGAGATCATATTCATATTCTCTGAG

For plasmid transfection, PEI MAX (Polysciences Inc.) was utilized following the dictates of the US patent application (number US20110020927A1) with minor modifications. Briefly, 16 hours before transfection, 2×10^6 cells were seeded on a 6-cm dish and then incubated. Expression vectors (3μg) and PEI MAX (1 mg/ml in 0.2 M HCl, 9μl) were preincubated for 20 min at RT in 0.5 ml solution [20 mM $CH_3CH(OH)COONa$ buffer and 150 mM NaCl at pH 4.0]. After incubation for 6 h, the transfection medium was replaced with a new standard culture medium for a further 48 h. For siRNA transfection, scramble and human BRCC36 siRNA-1 (CAUAAUGGCUCAGUGUUUA), human BRCC36 siRNA-2 (CGUCAGAAUUGUUCACAUU), mouse BRCC36 siRNA-1 (CAUAAUGGCUCAGUAUUUA), mouse BRCC36 siRNA-2 (GAACGGAAAUGCGCACAGU) (synthesized from the horizon, Tokyo, Japan) were transiently transfected into the cells by lipofectamine 2000 reagent according to the

instructions. Other siRNA sequences are listed in Table 2.

Table 2. siRNA sequences

Gene names	siRNA-1 (5'-3')	siRNA-2 (5'-3')
SNX2	CCACAGAAGUUGUAUUAGA	UGAAUCGGAUGCAUGGUUU
TANC1	GAAGUUAAAGCACGAUUUG	UAAGUGCGCUGCCAUUUGU
SNX6	GAUGAAGACCUCAAACUUU	UAAAUCAGCAGAUGGAGUA
HSPA6	GAGGAAAGCCUUAGGGACA	GCACAGGUAAGGCUAACAA
AP3B1	GUGAUAAGAUGGUCUCUAU	GCAAUAGGGAGGUGCAGUA
TBC1D23	GCGCUGAAUUCUGUAGUUA	GUUGUGAUCUUGAAACGUU
CLINT1	GAUCACAGAAUACAGAUAU	GAUCAGAGCGUGUUGUUAC
SAR1A	GAGCAAGCACGUCGCGUUU	UUAAUGGGAUUGUCUUUCU
BRCC3	CAUAAUGGCUCAGUGUUUA	CGUCAGAAUUGUUCACAUU
PTPN1	GAUCGAAGGUGCCAAAUUC	GGAUUAAACUACAUCAAGA
CISD2	UCGCUAGGCUCACAGUUUC	CUGCAUAUCUGAAGCGGCU

2.4 Generation of CRISPR/Cas9-based GnT-I-KO cells

The GnT-I–KO PX458 plasmid (32) was electroporated into the 293T cells according to the manufacturer's instructions (Amaxa cell line Nucleofector kit; Lonza, Basel, Switzerland). After 1 day of transfection, GFP-positive cells were sorted using FACS Aria II (BD Bioscience). Approximately 7 d after that, FACS sorting was performed with L-PHA lectin to detect GnT-I deletion (KO). The cells with negative fluorescence were seeded in 96-well plates to get single clones and sequenced.

2.5 Real-time quantitative PCR

Cells were treated with TRIzol Reagent (Invitrogen) for RNA extraction, and then we used the PrimeScript RT reagent Kit with a gDNA Eraser kit (Takara) to synthesize cDNA. The target gene expression levels were detected via RT-PCR, and quantified data were normalized to GAPDH. The primers are listed in Table 3.

Table 3. Primer sequences for RT-PCR

Gene names	Sense (5'-3')	Antisense (5'-3')
m-BRCC36	CATCTTGAGTCTGACG	GACCTGTTAGTTCAGC
h-BRCC36	AGGAAGTAATGGGGCTGTGC	AGTTCAGCCAACCTCTCTGC

2.6 Immunoprecipitation and western blotting

For immunoprecipitation (IP), the cells were lysed in the lysate buffer and quantified. The indicated antibody was connected with 10 μl magnetic beads (ProteNova) for 2h at RT. After washing with TBS, the suspension of the magnetic beads-antibody complexes was mixed with lysed protein and incubated at 4 °C for 6 h

to allow the protein to bind with magnetic bead-Ab complexes. After washing with TBS, elution buffer was added to the tubes and boiled at 100 °C for 5 min to release the Ab-Ag complexes from magnetic beads. The supernatant containing the target protein was then used to perform a western blot to detect associated proteins. The same amounts of proteins were loaded to 10% SDS/PAGE gels and then were transferred onto a PVDF membrane (Millipore Sigma). After blocking with defatted milk, the membrane was incubated either with the primary and secondary antibodies or with the Vectastain ABC kit (Vector Laboratories). Immobilon western chemiluminescent HRP substrate (MilliporeSigma) was performed to analyze the samples.

2.7 Preparation of biotinylated peptides and mass spectrometry analysis

The cells in 10 cm dishes were treated with 50 mM biotin for 6 h and then were lysed in 6 M guanidine-HCl containing 100 mM HEPES-NaOH (pH 7.5), 10 mM Tris-phosphine (Sigma), and 40 mM chloroacetamide (Wako) (33). The cell lysates were boiled at 95 ℃ for 10 min, sonicated, and centrifuged at 20000 g for 15 min to recover the supernatants. The proteins were extracted by methanol-chloroform precipitation (34) and solubilized in lysis buffer [50mM EPPS with 1% SDC (deoxycholic acid sodium salt monohydrate, Nacalai, Japan) and 0.7% SLC (Sodium N-Dodecanoylsarcosinate, Wako)]. The amounts of proteins (1.5 mg) were digested with trypsin (10 μg/mg) (TRTPCK, Worthington, UK), Lysyl endopeptidase (5 μg/mg) (Wako), and Glu C (5 μg/mg) (Thermo) at 37 ℃ overnight. After digestion, the samples were boiled at 100 ℃ for 5 min to inactivate proteases and incubated with the streptavidin-coated magnetic beads (30 μl) (TAMAGAWA, Tokyo, Japan) at 4 °C overnight with rotation. After sequential washing with 2 M ammonium acetate in 10% acetonitrile, 10% acetonitrile, 2% SDS, and 10% acetonitrile, these biotinylated peptides were sequentially eluted with 1, 1, 1, 3, 3, 3-hexafluoro-2-propanol (HFIP, Nacalai, Japan) containing 10% water and 2% ammonium acetate at 37 °C. The eluates were evaporated to remove the HFIP and dissolved in 3% acetonitrile. Then, these samples were desalted using GL-Tip SDB (GL Sciences, Tokyo, Japan), evaporated, redissolved in 0.1% TFA and 3% acetonitrile, and finally applied to mass spectrometry analysis.

The LC-MS/MS analysis described used an EASY-nLC 1200 HPLC system to separate the peptides, which were then ionized by a nanoelectrospray ion source and analyzed using a Q Exactive mass spectrometer, both of which are made by Thermo Fisher Scientific. The separation of the peptides was achieved using a 75 μm inner diameter × 125 mm C18 reverse-phase column made by Nikkyo Technos NTCC-360. The separation was performed using a linear gradient of acetonitrile with 0.1% formic acid, starting at 5% and increasing to 40% over 60 minutes, followed by a further increase to 95% acetonitrile during the next 10 minutes (60-70 min). The resulting peptides were then analyzed using tandem mass spectrometry (MS/MS) to identify the peptides and the proteins they originated from. This technique is commonly used in proteomics research to identify and quantify proteins in complex biological samples (35,36).

The Q Exactive mass spectrometer used in the LC-MS/MS analysis was operated in data-dependent acquisition (DDA) mode with a top 10 MS/MS method. The top 10 most intense precursor ions in each MS1 scan were selected for fragmentation and subsequent MS/MS analysis. The MS1 spectra were acquired with a resolution of 70,000, an AGC target of 1e6, and a mass range from 350 to 1500 m/z. HCD (higher-energy collisional dissociation) MS/MS spectra were acquired at a resolution of 17,500, an AGC target of 5e4, and an isolation window of 2.0 m/z. The maximum injection time for the HCD MS/MS spectra was set to 200ms, and the normalized collision energy was set to 27. Dynamic exclusion was set to 15 s, which means that any precursor ion selected for MS/MS analysis was excluded from selection for the next 15 s to prevent repeated selection of the same precursor ion. These parameters were chosen to maximize the analysis's sensitivity and specificity and minimize the possibility of false identifications.

2.8 Immunofluorescent staining

Cells cultured on glass bottom dishes were fixed in 4% paraformaldehyde for 30 min, followed by incubating with 0.1% TritonX-100 in PBS for 20 min. Next, cells were blocked with 5% bovine serum albumin (BSA) to decrease nonspecific staining.

Cells were then incubated overnight with antibodies as indicated at 4 °C, followed by incubation with the secondary antibody and DAPI. Fluorescence was detected via LSM 900 Laser Scanning microscope with Axio Observer and ZEN 3.0 software.

2.9 Assay for protein stability

Analysis of FLT3 stability was carried out using CHX or MG132. The 293T cells transfected with FLT3-WT, FLT3-ITD, or FLT3-TKD were cultured with or without 50 μg/ml CHX or 5 μM MG132 at indicated times. The band densities of FLT3 and α-tubulin were obtained from each scanned western blot. Normalization was performed by the α-tubulin signal at each time point to get the FLT3 level histogram.

2.10 Cell apoptosis assay

Ba/F3 cells were cultured in the normal culture condition for 24 h, then treated with or without thiolutin and/or quizartinib for 6 h. The cell apoptosis assay was performed by flow cytometry using a FITC-conjugated Annexin V kit (37) according to the manufacturer's instructions (MBL, Japan).

2.11 Statistical analysis

GraphPad Prism® 6.0 software (GraphPad Software, CA, USA) was used for statistical analysis, and results are reported as the means ± SD. To analyze differences between groups, one-way ANOVA or independent-samples t-test was performed, and the statistical significance was indicated as follows, n.s, no significance, $*p < 0.05$, $**p < 0.01$, and $***p < 0.001$.

3. Results

3.1 Comparison of FLT3 localization in FLT3-WT, FLT3-ITD, and FLT3-TKD cells

It has been known that there are two forms of human FLT3; one is a mature form at around 150 kDa, which is thought to be fully N-glycosylated and is then expressed on the cell surface to activate MAPK signaling pathways efficiently. The other is an immature form at around 130 kDa, which may be mainly localized in the ER (38) as shown in Figure 1. To confirm further the difference in the mature status of FLT3-WT and mutants, we transfected 293T cells with corresponding plasmids and performed western blotting. There was a more mature form in FLT3-WT cells than in mutant cells. In FLT3-ITD, most of the protein was immature, with a small percentage of mature form, while FLT3-TKD mainly existed as an immature form (Figure 2A). Changes in FLT3 localization are known to affect downstream signaling (39). To determine the specific location of FLT3, the immunostaining used antibodies against FLT3, and calnexin, an ER marker, was performed in HeLa cells. Consistent with previous results, FLT3-WT was mainly located on the cell surface, while ITD was mainly localized in the ER, co-localized with calnexin staining, and a fraction of them were localized on the cell surface. Almost all TKD proteins were localized in the ER (Figure 2B). Previously, we found that FLT3-ITD and TKD also have the complex N-glycans containing fucosylation (27), which are synthesized and processed in the Golgi apparatus.

Considering both mutants are mainly located in ER as previously described (40) as well as in the present study, we speculate that both mutants may be transported to the Golgi apparatus once and then undergo retrograde transport from Golgi to ER to activate the downstream pathways. Therefore, we performed the immunostaining to check if ITD and TKD were also localized in the Golgi apparatus. These mutants were partly co-localized with GM130, a cis Golgi marker (Figure 2C). ITD and TKD can induce a robust activation of STAT5. We found that the Golgi entry was essential for these mutants-mediated cellular signaling. As shown in Figure 2D, p-STAT5 levels

were significantly suppressed in these mutants in the presence of brefeldin A (BFA), which blocks the ER-Golgi transport (41). Furthermore, p-STAT5 levels were also significantly suppressed in GnT-I KO cells (Figure 2E), suggesting that the complex type of N-glycans processed in the Golgi apparatus is essential for these FLT3 mutants-mediated signaling.

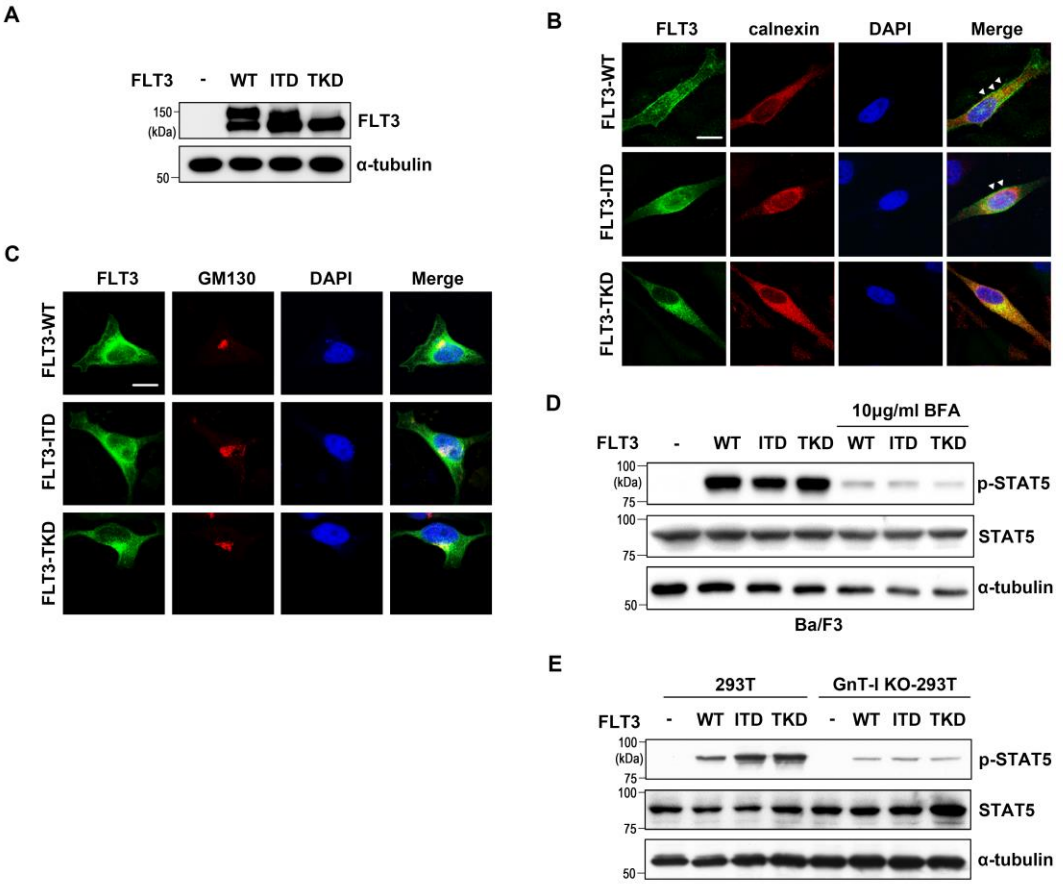

Figure 2. Comparison of FLT3 localization among WT and mutants in HeLa cells, and effects of N-glycosylation on cellular signaling. (A) Expression patterns of FLT3 in 293T cells. Expression of WT, ITD, or TKD was determined by western blotting with FLT3 antibody. (B) and (C) Representative images of immunofluorescent staining with indicated antibodies showed the expression and localization of WT, ITD, and TKD (green) in HeLa cells, in which ER and Golgi apparatus (red) are more easily distinguishable due to the superior cell spread property compared to other cell types such as 293T and Ba/F3 cells. The white triangles indicate the cell surface area. DAPI (blue) was used for nuclear staining. Bar represents 20 μm. (D) The levels of p-STAT5

were analyzed by western blot in Ba/F3 cells treated with or without BFA. (E) Effects of GnT-I-KO on the levels of p-STAT5 in 293T cells. The same amounts of cell lysates were blotted with indicated antibodies. α-tubulin was used as an internal control.

3.2 Comparison of protein stability of FLT3 among the three cell lines

In addition to localization, we also investigated the protein stability of WT and FLT3 mutants in 293T cells. When cells were treated with MG132, a proteasome inhibitor, the increase of FLT3 was observed only in the WT cells, compared with the ITD and TKD cells (Figure 3A), suggesting the degradation of both mutants is mainly not through the proteasomal pathway. On the other hand, when cells were treated with CHX, a protein synthesis inhibitor, the decay of FLT3 in the WT or ITD cells was significantly faster than that in TKD cells (Figure 3B), which suggests that TKD is more stable than ITD in some extent. The two mutants' different locations and protein stabilities further prompted us to investigate the underlying mechanisms.

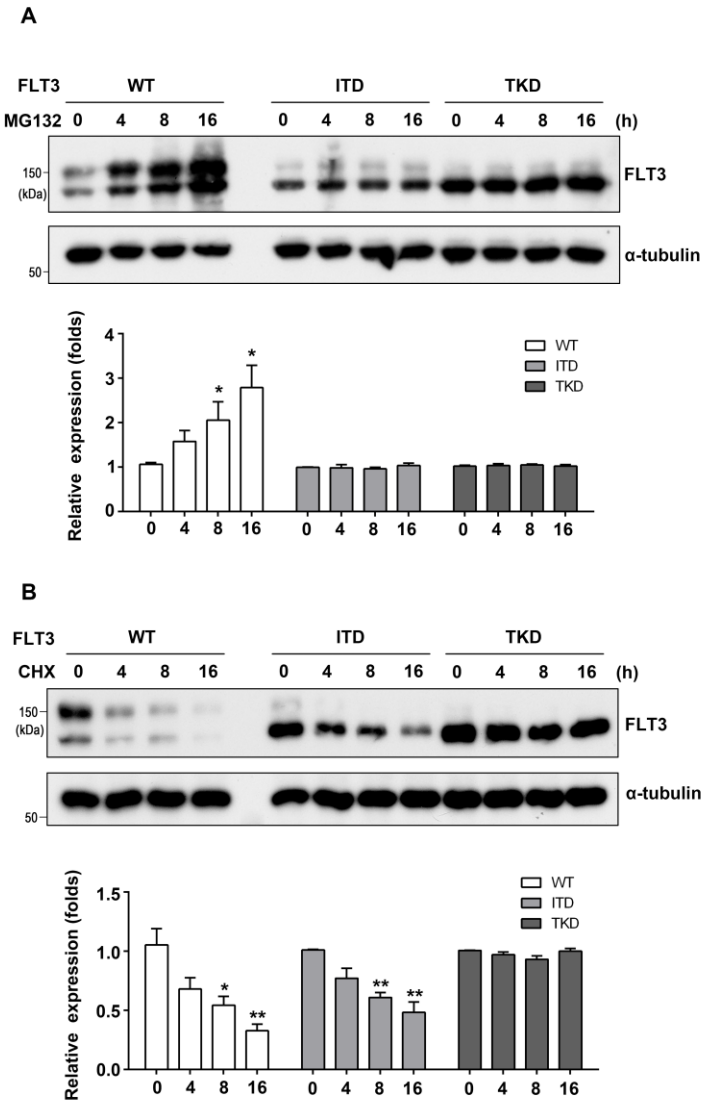

Figure 3. Comparison of FLT3 stabilities among WT and mutants. 293T cells were transfected with WT, ITD, or TKD and then treated with MG132 (A) or CHX (B) for indicated times. The same amounts of cell lysates were blotted with indicated antibodies. The experiments were independently repeated three times. α-tubulin was used as an internal control. The intensities of FLT3 calculated the relative intensities to that of α-tubulin. The ratio in cells without MG132 or CHX was set as 1.0. Data were analyzed by one-way ANOVA and presented as the mean ± SD. *$p < 0.05$, **$p < 0.01$.

3.3 Proximity labeling and identification of proteins that specifically interact with FLT3 mutants

To identify proteins that differently regulate FLT3-ITD or FLT3-TKD, we

performed the strategy of proximity labeling with TurboID fused to the C-terminus of FLT3, which catalyzes the biotinylation of proteins that transiently interact with FLT3 in the presence of biotin. Considering the higher transfection efficiency and protein yield, we transfected these expression vectors into 293T cells. Western blotting with anti-FLT3 antibody demonstrated that FLT3-TurboID was successfully expressed, and the two forms of FLT3 shown in Figure 4A were quite similar to the pattern as shown in Figure 2A without the TurboID tag, suggesting that the TurboID tag does not affect the location of FLT3 proteins and the posttranslational modification by N-glycans.

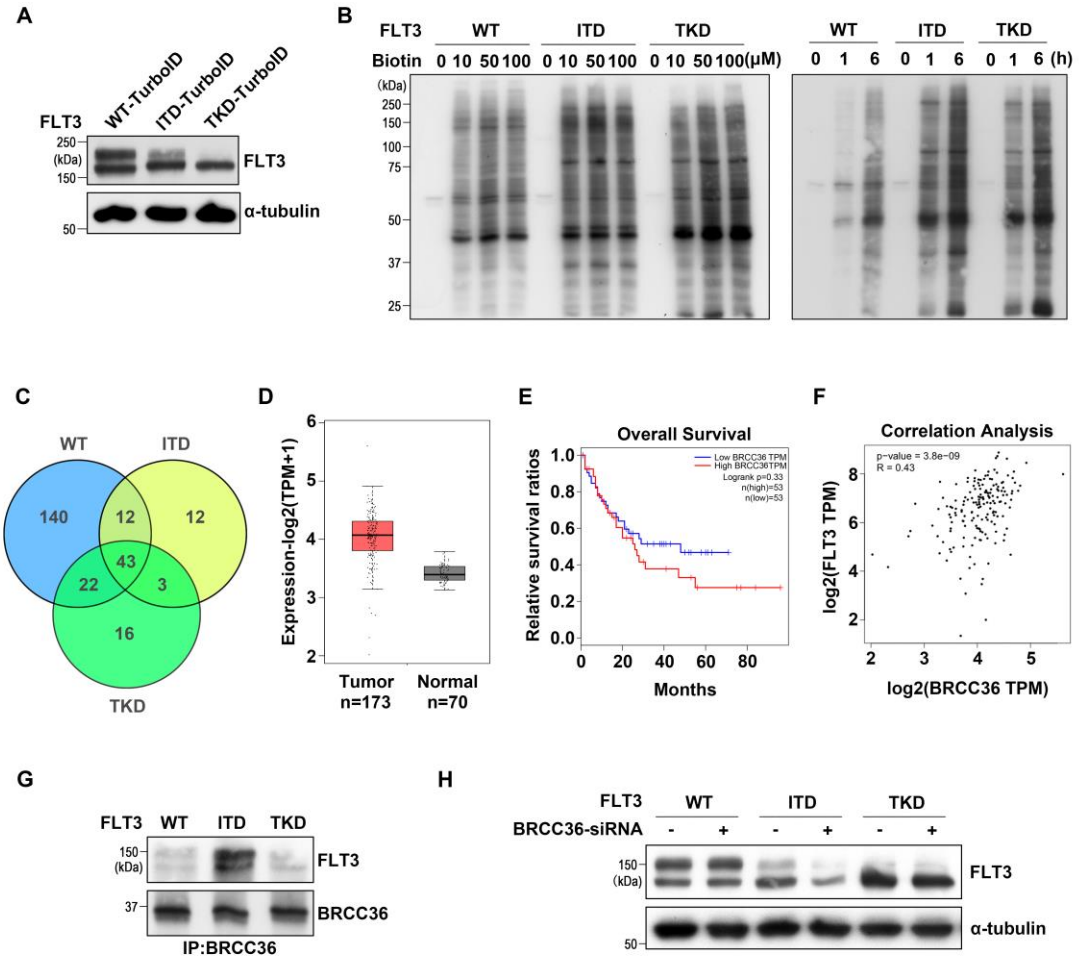

Figure 4. Proximity labeling and identification of BRCC36. (A) Expression patterns of FLT3-TurboID in 293T cells. Expression of WT-, ITD-, or TKD-TurboID was determined by western blotting with FLT3 antibody. (B) Determination of suitable biotin concentration and labeling time in 293T cells expressing WT-, ITD-, or TKD-TurboID. The same amounts of cell lysates were detected with the ABC kit. (C) Venn

diagram showing the peptide distribution identified by MS in 293T cells expressing WT-, ITD-, or TKD-TurboID. After biotinylation, the peptides were purified by the streptavidin-coated magnetic beads as described in "**Materials and methods**" (D) Expression levels of BRCC36 in AML and normal tissues in the GEPIA database (n = 243). TPM, transcripts per million. (E) Survival plots of AML patients were stratified by the BRCC36 levels using the GEPIA database (n = 106). The vertical lines represent censored data. (F) Correlation analysis between FLT3 and BRCC36 gene from GEPIA database. (G) The immunoprecipitates (IP) with anti-BRCC36 antibody were analyzed by western blot using an anti-FLT3 antibody. (H) 293T cells were transfected with WT, ITD, or TKD plasmids with or without BRCC36-siRNA. FLT3 stability was evaluated by western blot using an anti-FLT3 antibody. α-tubulin was used as an internal control.

To identify the optimal biotin concentration for protein labeling, we treated cells with varying concentrations of biotin and found that 50 μM is sufficient for biotinylation (Figure 4B left panel). We treated the cells with 50 μM biotin for varying durations to determine the optimal incubation time (Figure 4B right panel). A 6-hour incubation was sufficient to achieve robust protein labeling. After the biotinylated proteins were digested by trypsin and affinity-purified by streptavidin beads, eluates were subjected to MS analysis as described above. 371 proteins were identified from FLT3-WT, ITD, and TKD samples. The visualized graph showed that 12 proteins were detected explicitly in ITD, and 16 were in TKD (Figure 4C). We selected 11 candidates detected exclusively in ITD or TKD related to protein stability, vesicle transport, or signal transduction. The effects of these 11 proteins were assessed by observing changes in the phosphorylation levels of STAT5, Erk, and Akt in FLT3-WT, ITD, or TKD cells, using specific siRNAs for each to exclude unrelated candidates (Figure 5). Among them, we noted that depletion of BRCC36, which was explicitly associated with ITD based on the MS results, significantly suppressed p-STAT5 and p-Erk in ITD cells, not TKD cells. Therefore, we considered BRCC36 as a potential ITD-interacting protein.

BRCC36 is a catalytic subunit responsible for most K63-Ub-specific DUB activity in the cytoplasm and the nucleus (42). The expression levels of BRCC36, survival rates in AML patients, and correlation analysis were obtained from the Gene Expression Profiling Interactive Analysis (GEPIA) database (http://gepia.cancer-pku.cn/). The data revealed marked upregulation of BRCC36 in the tumor group compared to that in the healthy group (Figure 4D), and BRCC36 caused a slight reduction of survival rate in AML (Figure 4E). Moreover, the expression of FLT3 is significantly correlated with the expression of BRCC36 (Figure 4F). To verify the MS results biochemically, we performed co-immunoprecipitation (Co-IP) experiments and found that BRCC36 specifically interacts with ITD (Figure 4G). Moreover, BRCC36-knockdown (KD) using siRNA destabilized ITD but not WT and TKD (Figure 4H). Collectively, the interaction between BRCC36 and FLT3-ITD is specific and functional.

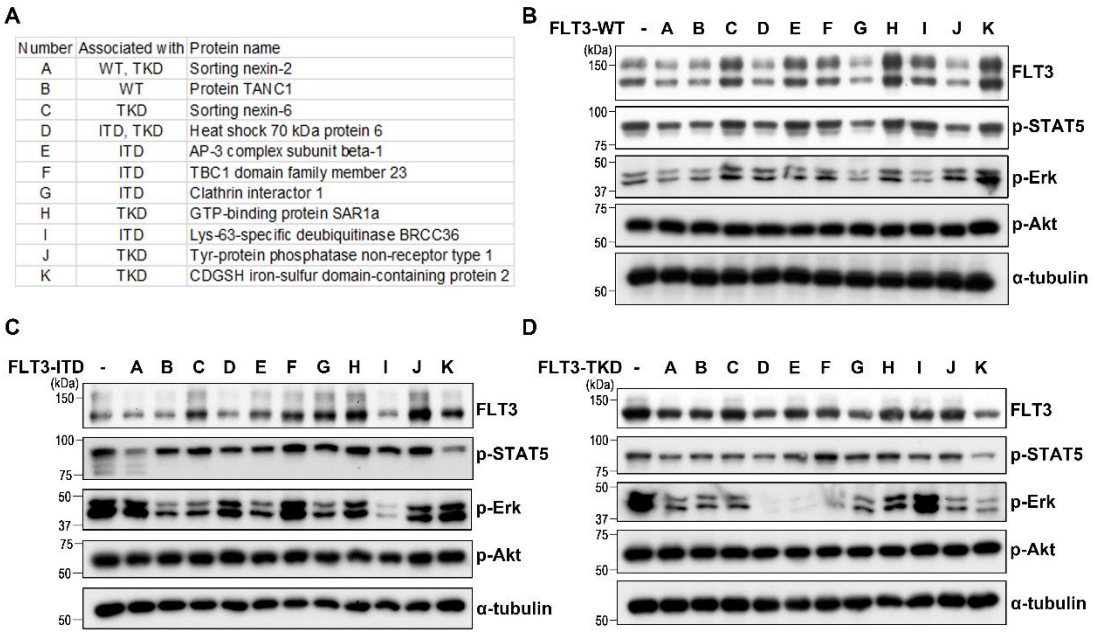

Number	Associated with	Protein name
A	WT, TKD	Sorting nexin-2
B	WT	Protein TANC1
C	TKD	Sorting nexin-6
D	ITD, TKD	Heat shock 70 kDa protein 6
E	ITD	AP-3 complex subunit beta-1
F	ITD	TBC1 domain family member 23
G	ITD	Clathrin interactor 1
H	TKD	GTP-binding protein SAR1a
I	ITD	Lys-63-specific deubiquitinase BRCC36
J	TKD	Tyr-protein phosphatase non-receptor type 1
K	TKD	CDGSH iron-sulfur domain-containing protein 2

Figure 5. Assessment of 11 candidates from MS data in 293T cells. We selected 11 proteins from MS analysis related to protein stability, vesicle transport, or signal transduction. (A) Information of the candidates. The protein names and correlations with FLT3 were listed. The effects of these 11 proteins on FLT3 were checked by changes in the phosphorylation levels of STAT5, Erk, and Akt in WT (B), ITD (C), or TKD (D) cells using respective specific siRNAs. α-tubulin was used as an internal control.

3.4 Effects of BRCC36 on cellular signaling and cell proliferation in FLT3-ITD-expressing cells

To investigate the influence of BRCC36 on FLT3 expression and cellular signaling, the BRCC36-siRNAs were transfected into both Ba/F3 cells and 293T cells. The efficiency of RNA interference was confirmed by qPCR (Figure 6A) and western blotting with an anti-BRCC36 antibody (Figure 6B, C). These siRNAs efficiently silenced the corresponding protein expression in both Ba/F3 and 293T cells and were used in the following experiments. In the BRCC36-KD Ba/F3 cells, the p-STAT5 levels and specific signaling of FLT3 were remarkably reduced in ITD cells compared to untreated cells. In contrast, the p-STAT5 levels in the WT or TKD cells were not affected by the BRCC36-KD (Figure 6B).

Furthermore, to confirm the influence of BRCC36 on FLT3, we transfected 293T cells with either BRCC36-siRNA or a BRCC36-overexpression plasmid. Consistent with the Ba/F3 cells data, BRCC36-KD attenuated the p-STAT5 levels only in ITD cells, not TKD-expressing 293T cells (Figure 6C). Conversely, overexpression of BRCC36 increased the FLT3 expression and enhanced the p-STAT5 levels in ITD cells, which were not observed in the TKD cells (Figure 6D). Moreover, we examined the effect of BRCC36-KD on the cell proliferation of Ba/F3 cells. The BRCC36-KD significantly inhibited cell proliferation of ITD cells but not WT and TKD cells (Figure 6E). These results further support the conclusion that BRCC36 regulates the expression and cellular signaling of the FLT3-ITD mutant.

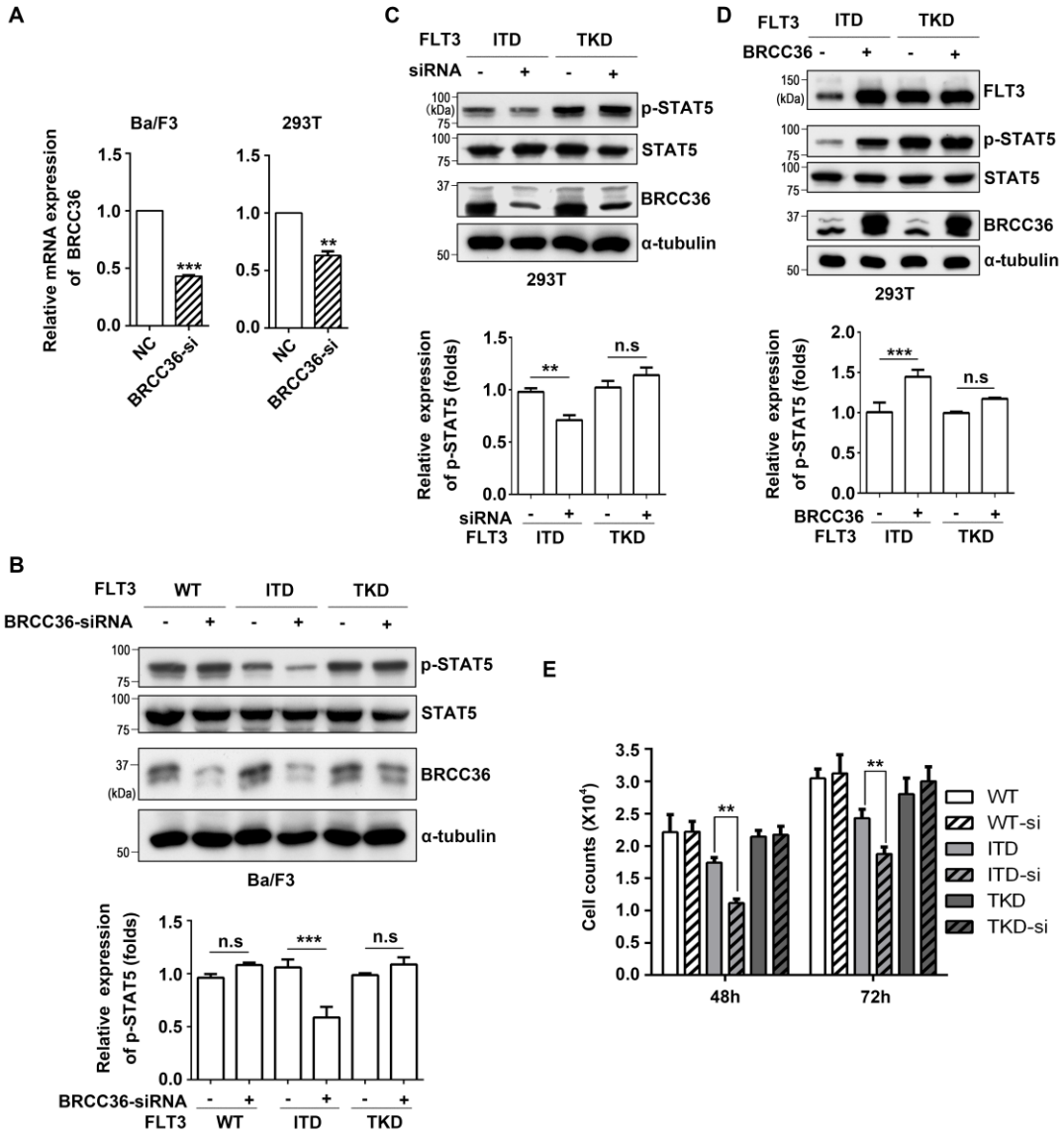

Figure 6. The effects of BRCC36 on FLT3 expression and its mediated signaling. (A) Ba/F3 cells and 293T cells were transiently transfected with BRCC36-siRNAs for 48 h, and then BRCC36 expression levels were detected by qPCR. GADPH was used as an internal control. After transfection with BRCC36-siRNAs, the expression levels of p-STAT5 and BRCC36 in Ba/F3 cells (B) or 293T cells (C) were detected by western blot using indicated antibodies. α-tubulin was used as an internal control. The intensities of p-STAT5 calculated the relative intensities to that of STAT5. The ratio in cells without transfection was set as 1.0. Data were analyzed by one-way ANOVA and presented as the mean ± SD (n=3). (D) After overexpression of BRCC36 in 293T cells, the expression levels of FLT3, p-STAT5, and BRCC36 were detected by western blot.

(E) Effects of BRCC36-siRNA on cell proliferation in WT, ITD, and TKD Ba/F3 cells. The experiments were independently repeated three times. $^{**}p < 0.01$, $^{***}p < 0.001$.

3.5 Effects of BRCC36 on the K63-linked polyubiquitin on FLT3-ITD

BRCC36 is a metalloprotease that specifically cleaves K63-linked polyubiquitin chains, so we wondered about the impact of the K63-ubiquitin chain on FLT3-ITD expression. 293T cells were co-transfected with the plasmids expressing each variant of FLT3 and HA-K63-Ub, a ubiquitin construct in which all lysine ubiquitination sites except K63 are mutated (31). Western blot analysis showed that K63-Ub containing HA tag was appreciably detected by the anti-HA antibody (Figure 7A). Following transfection with K63-Ub, the expression levels of FLT3 in ITD cells were significantly decreased compared to those in TKD cells (Figure 7A). To confirm the interaction between BRCC36 and ITD further, the cells expressing HA-K63-Ub and ITD or TKD were treated with or without thiolutin (Thl), which is characterized as a Zn^{2+} ion chelator capable of inhibiting DUB activity, including BRCC36 (43). Western blot results showed that thiolutin significantly downregulated the p-STAT5 levels in both Ba/F3 cells and 293T cells expressing ITD, not those expressing WT or TKD (Figure 7B, C). The Co-IP revealed that inhibition of BRCC36 induced more K63-Ub chains in ITD cells compared with the control cells (Figure 7D), while no changes were observed in the TKD cells (Figure 7D). These data suggest that BRCC36 disassembles the K63-linked polyubiquitin chains on FLT3-ITD, thereby increasing protein stability.

Given the interaction between BRCC36 and FLT3-ITD, we determined the specific ubiquitination site to understand why BRCC36 cleaved K63-Ub specifically in ITD but not in TKD. Ubiquitination starts with connecting a single ubiquitin molecule to a substrate lysine residue (4). Considering the molecular features of two mutants, we speculated that lysine 609 of ITD located in the juxtamembrane domain (a specific duplication insertion region) (19,44), might be a potential ubiquitination site. To determine the importance of this lysine residue in ITD for K63-Ub binding, we utilized the ITD mutant in which this lysine residue was substituted with arginine (FLT3-ITD-

K609R) (Figure 7E). As expected, IP experiments demonstrated that the K63-Ub levels were suppressed in the FLT3-ITD-K609R cells (Figure 7F). Furthermore, the interaction with BRCC36 decreased in the ITD-K609R cells (Figure 7F). These data indicate that K609 of FLT3-ITD is a critical site for K63 ubiquitination. Consistently, the expression levels of ITD were enhanced in the ITD-K609R cells (Figure 7G), suggesting the K63-Ub promotes ITD degradation.

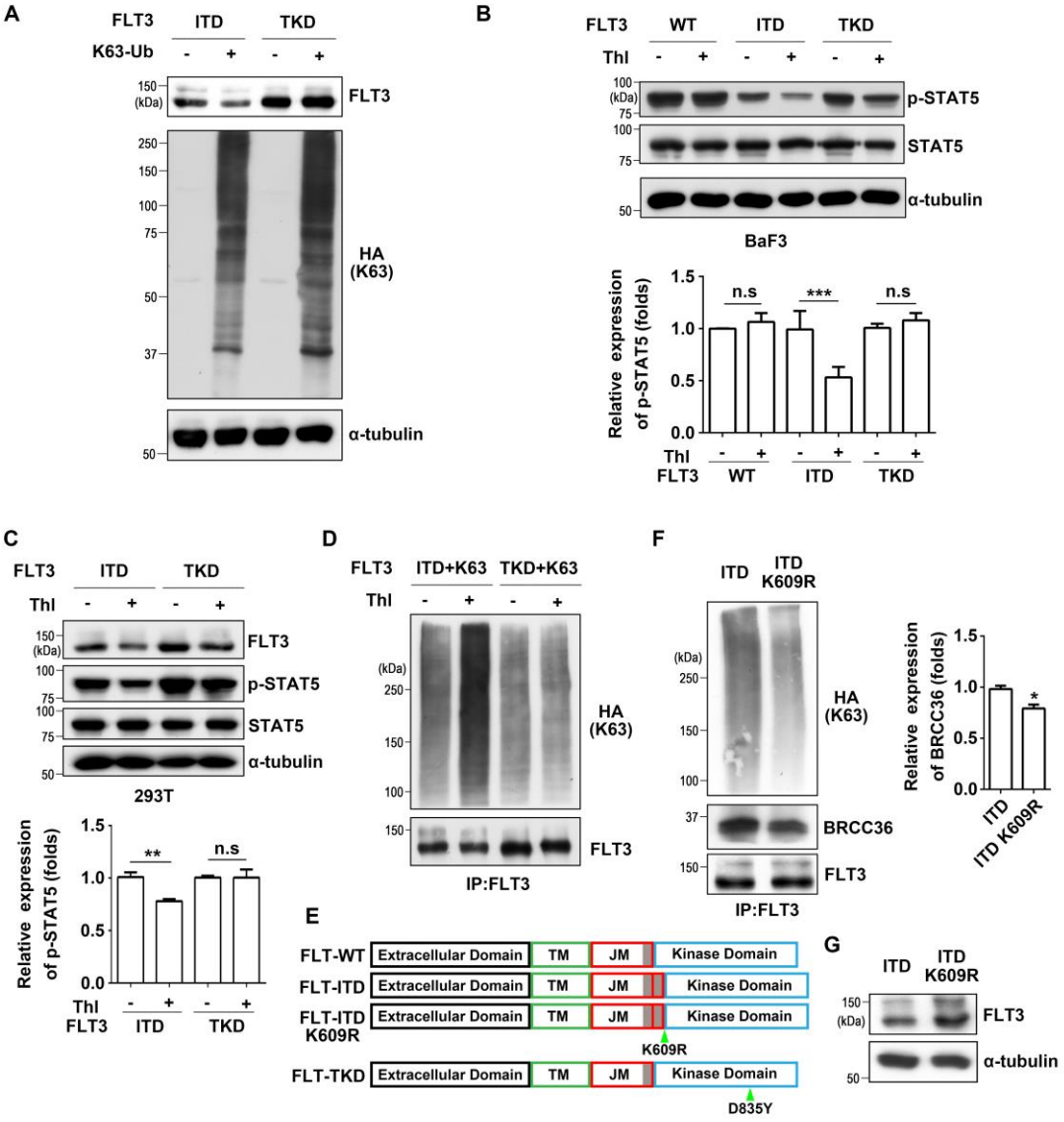

Figure 7. Thiolutin, a BRCC36 inhibitor, affects FLT3-mediated signaling and K63 polyubiquitin. (A) 293T cells were transfected with HA-K63-Ub and ITD or TKD. The expression levels of FLT3 and HA-K63-Ub were detected by western blot using anti-FLT3 and anti-HA antibodies. After treatment with thiolutin (Thl), the expression levels of FLT3 and p-STAT5 in Ba/F3 cells (B) or 293T cells (C) were detected by

western blot. The relative intensities were calculated by the intensities of p-STAT5 to that of STAT5. The ratio in cells without treatment with Thl was set as 1.0. Data were analyzed by one-way ANOVA and presented as the mean ± SD (n=3). α-tubulin was used as an internal control. (D) 293T cells expressing HA-K63-Ub and FLT3-ITD or TKD were treated with or without thiolutin. After immunoprecipitation with an anti-FLT3 antibody, the expression levels of K63 polyubiquitin in the immunoprecipitants were detected by western blotting with an anti-HA antibody. (E) The diagrams show WT and mutants used in this study. The grey shadow shows the REYEYDL(K) amino acid sequence, which is duplicated in the ITD. TM, transmembrane domain; JM, juxtamembrane domain. (F) The effects of lysine at 609 of ITD on K63 polyubiquitin and interaction between ITD and BRCC36. The immunoprecipitants of FLT3 were detected by western blotting with indicated antibodies. The relative intensities were calculated by the intensities of BRCC36 against FLT3. The ratio in ITD cells was set as 1.0. (G) The expression levels of FLT3 in the same amounts of cell lysates were evaluated by western blot. α-tubulin was used as an internal control. *$p < 0.05$, **$p < 0.01$, ***$p < 0.001$.

3.6 Synergistic effects of BRCC36 inhibitor and FLT3 kinase inhibitor on FLT3-ITD-mediated cellular signaling, cell proliferation, and cell apoptosis

To explore the function of thiolutin in the treatment of AML, we treated the cells with or without thiolutin and/or AC220 (quizartinib), a tyrosine kinase inhibitor with clinical promise for AML (45). The combination of the two drugs efficiently reduced the expression levels of p-STAT5 (Figure 8A) and exhibited robust antiproliferative potencies in FLT3-ITD Ba/F3 cells (Figure 8B). Furthermore, an Annexin V-FITC apoptosis assay revealed that the combination of drugs significantly induced cell apoptosis (Figure 8C). To further investigate the specific role of thiolutin in leukemia cells, we utilized human leukemia cell lines MV4-11 and RS4-11, which endogenously express similar levels of FLT3-ITD or FLT3-WT, respectively (46). As expected, the cell viability assay showed that MV4-11 cells were more sensitive to the stimulation of

thiolutin than RS4-11 cells (Figure 8D). Taken together, our data suggest that the potential synergistic activity of the dual inhibition of FLT3/BRCC36 may apply to the clinical treatment of FLT3-ITD patients.

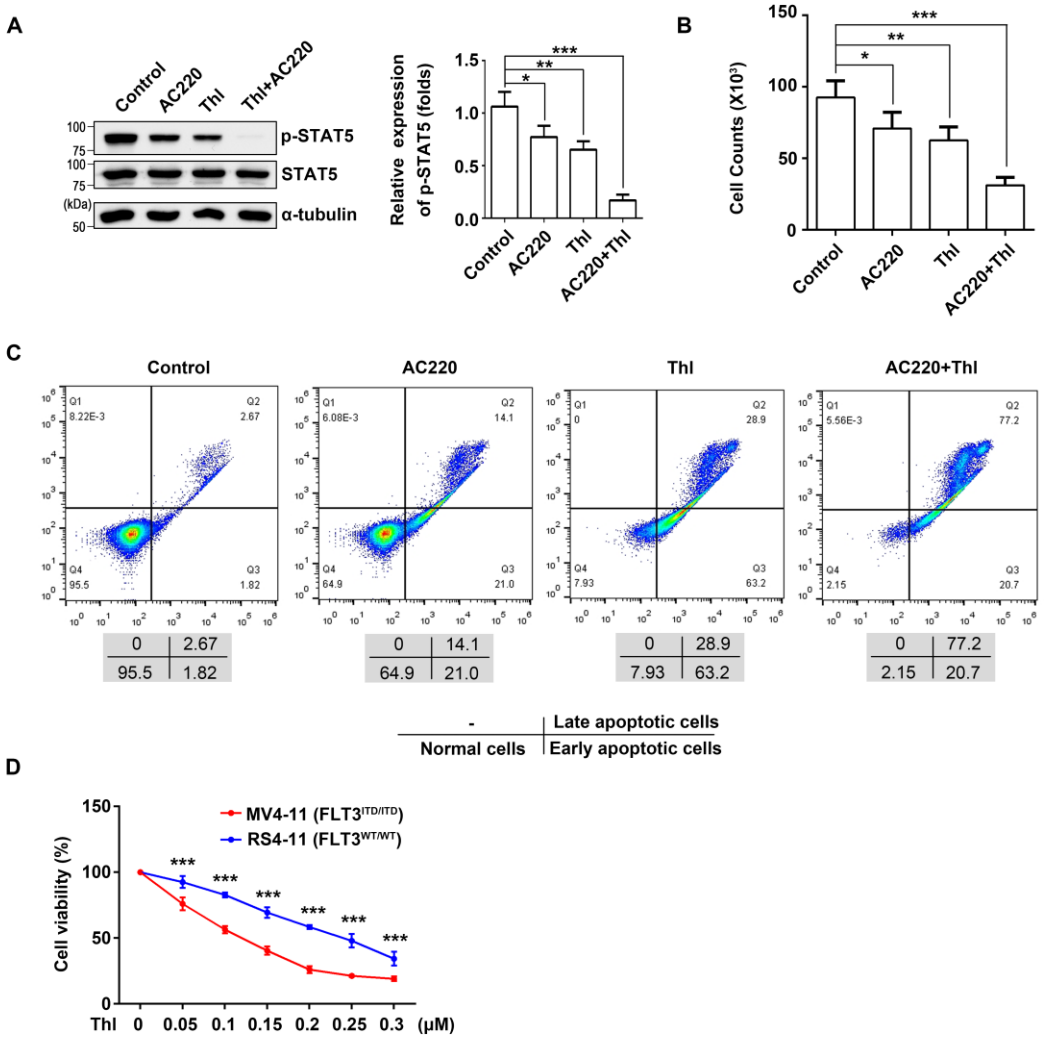

Figure 8. Synergistic inhibitory effects of thiolutin and quizartinib on cellular signaling, cell proliferation, and apoptosis in FLT3-ITD Ba/F3 cells. (A) The expression levels of p-STAT5 in ITD cells, following various treatments, were detected by western blot. α-tubulin was used as an internal control. The relative intensities were calculated by the intensities of p-STAT5 against STAT5. The ratio in cells without treatment with the drug was set as 1.0. Data were analyzed by one-way ANOVA and presented as the mean ± SD (n=3). These treatments also affected cell proliferation abilities using cell counting (B) and cell apoptosis using Annexin V-FITC apoptosis assay kit (C). (D) MV4-11 cells (FLT3-ITD positive) and RS4-11 cells (FLT3-ITD

negative) were treated with different doses of thiolutin, and a cell viability assay was performed to determine the drug sensitivity. The number of cells without the treatment was set as 100%. *$p < 0.05$, **$p < 0.01$, ***$p < 0.001$.

4. Discussion

In this study, we screened for proteins that interact with FLT3 mutants and found that BRCC36, a K63-linked polyubiquitin chain deubiquitinase, was specifically associated with FLT3-ITD and increased its stability and downstream signaling (Figure 9). Conversely, the downregulation of BRCC36 expression or BRCC36 activity suppressed the downstream signaling and cell proliferation and promoted cell apoptosis. These results suggest that BRCC36 may be a potential therapeutic target protein for AML.

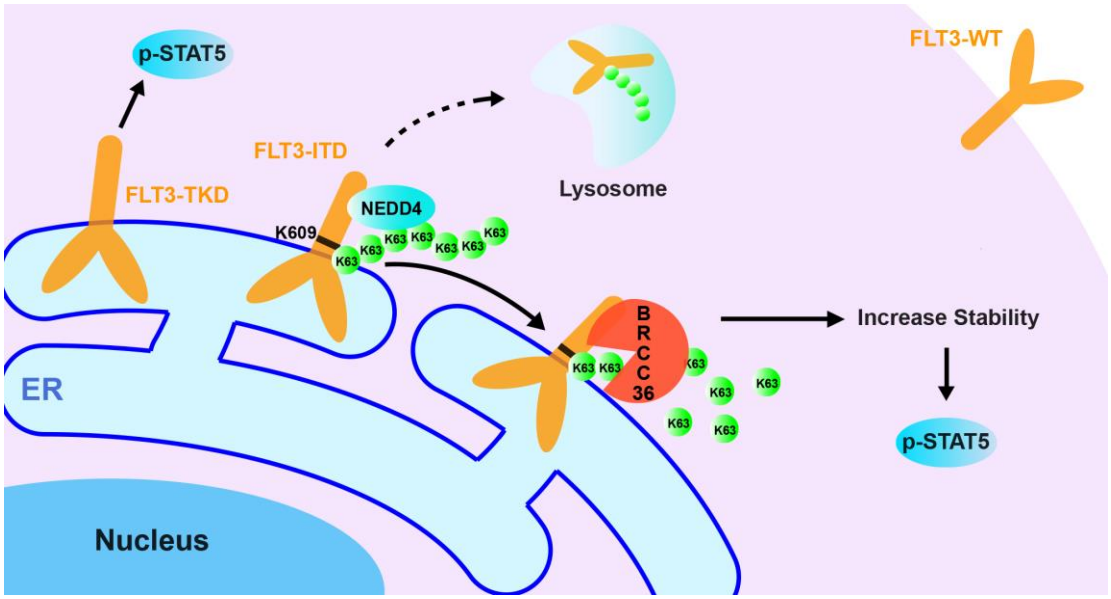

Figure 9. Schematic diagram of the proposed molecular mechanism for the specific interaction between FLT3-ITD and BRCC36 for regulating cell functions. FLT3 is one of the most frequently mutated genes in AML, such as ITD and TKD, which shift the localization on the cell surface to ER, where both activate STAT5. Most patients harboring ITD mutants suffer from a worse relapse and poor survival rates. This study demonstrates that BRCC36, a K63-linked polyubiquitin chain deubiquitinase, was selectively associated with ITD, not WT or TKD, enhancing its stability and downstream signaling, including p-STAT5. Furthermore, we identified that K609, which links with the duplicate sequence in ITD, is a critical site for K63-linked polyubiquitin, which is presumably modified by NEDD4 (47). Thus, BRCC36 may be a promising target for novel therapy against FLT3-ITD-positive AML.

FLT3 is a transmembrane ligand-activated receptor tyrosine kinase commonly expressed in hematopoietic stem cells and plays a vital role in the early stages of myeloid and lymphoid lineage development (48). FLT3-ITD occurs as the replicated sequence in the juxtamembrane domain, and TKD occurs in the tyrosine kinase domain. Both mutants constitutively activate FLT3 kinase activity, thereby playing a role in the biology of AML. The present study showed that both have different N-glycosylation patterns and intracellular localizations (Figure 2). This is consistent with previous studies that noted most ITD and TKD are localized at the ER, with only a minority of ITD expressed on the cell surface (49,50). It is worth noting that although both are mainly located in the ER, entry into the Golgi for further N-glycosylation is essential for cellular signaling mediated by both mutants. This is because blocking ER-Golgi transport with BFA or GnT-I-KO significantly suppressed p-STAT5 levels (Figure 2). In addition, both mutants showed distinctive protein stabilities, i.e., TKD is more stable than ITD (Figure 3). These studies suggest that both mutants may have different regulatory mechanisms in AML biology.

Compared with TKD, patients harboring ITD have elevated peripheral blood counts, an increased chance of relapse, and inferior overall survival (19). In experimental models, ITD induced a myeloproliferative phenotype for myeloproliferative disease, whereas TKD caused a lymphoid disease with different hematologic manifestations in the murine bone marrow (25,51). Both mutants differ concerning their structural features and clinical presentation but also show significant disparities in biological transforming potential and molecular biology, as described above. Thus, exploring the target protein collaborating with ITD or TKD specifically for treating AML is fundamental.

Traditional techniques for identifying protein interaction face challenges in effectively capturing weak or transient interactions. In this study, we used the TurboID ligase (29), a new proximity-dependent labeling technique, to identify target proteins associated with FLT3. According to the results of MS analysis, BRCC36, a

deubiquitinase for K63 polyubiquitination, was found to be explicitly associated with ITD, not TKD or WT. Furthermore, using biochemical approaches, this study proved that ITD physically and functionally interacts with BRCC36 (Figures 4-8). It has been reported that ITD could be poly-ubiquitinated in both K48-linked and K63-linked, and the K48 polyubiquitination was preferentially linked by c-Cbl (47), while neural precursor cell-expressed developmentally downregulated protein 4 (NEDD4) preferentially performed K63 polyubiquitination, an E3 ligase reported specific for K63 chains (52). Interestingly, inhibition of the deubiquitinase USP9X, which cleaves various Ub chains, including K48 and K63 linkages, induced apoptosis preferentially in cells transformed by ITD mutant and decreased the downstream signaling event (53). In addition, inhibiting deubiquitinase USP10, which cleaves K48 linkage, promotes ITD degradation and confers an anti-proliferative effect both in vitro and in vivo (54). Although those studies did not show the direct interaction between DUBs and FLT3, they underscored the importance of regulatory polyubiquitination in playing crucial roles in the pathological phenotypes of ITD, which further supports our findings. Our results revealed that BRCC36 specifically and spatially connects with FLT3-ITD and disassembles its K63-ubiquitin. This might provide more precise insights into the molecular mechanisms and evidentiary support for the significance of K63-ubiquitin in regulating ITD in hematopoietic cells. To understand why BRCC36 cleaved K63-Ub specifically in ITD but not in TKD, we established FLT3-ITD-K609R cells according to the different molecular features of two mutants (Figure 7E) and performed IP experiments with these cells. The data indicated that K609 of ITD is a critical site for K63 ubiquitination. Furthermore, the interaction with BRCC36 was diminished in ITD-K609R cells compared to ITD cells, suggesting that the interaction with BRCC36 may depend on the duplicate sequence of ITD.

It has been reported that K63-linked polyubiquitination may lead to the degradation of a protein by a lysosomal pathway, not proteasomal degradation (9,55). Our study suggests that ITD might undergo degradation via the lysosomal pathway rather than the proteasomal pathway, as evidenced by the stability of ITD in the early

phase (16 h) not being affected by MG132 (Figure 3A). However, we cannot entirely exclude the possibility of ITD degradation via the proteasome system, as the K48-linked chain modifies it (47). On the other hand, the K63-linked chain was also reported to have a protective effect on some proteins. For instance, K63-ubiquitination promoted the stability and activation of Janus kinase 2 (JAK2) in the hematopoietic stem cells (56). The regulation of protein stability through K63-ubiquitination seems to depend on target proteins.

FLT3-ITD mutations are correlated with specific cytogenetic subgroups. Among acute promyelocytic leukemia (APL) patients with PML-RARα, it was reported that 30-50% of the patients had FLT3 mutations (57,58). Frequent (~90%) co-occurrence was reported in patients with t(6; 9) and FLT3-ITD mutations (57,59). Similarly, FLT3-ITD mutations are also frequently found in patients with mixed lineage leukemia (MLL)-partial tandem duplication (PTD) (60). The rate of MLL-PTD in FLT3-ITD-positive patients was significantly higher than that in FLT3-ITD-negative patients (60). Given that FLT3-ITD mutations have unique distributions among AML subtypes, we will analyze the distribution of BRCC36 in these subtypes to identify potential overlaps.

FLT3 inhibitors are widely used for the treatment of AML and significantly improve the survival and prognosis of AML patients (61). However, the efficacy of FLT3-targeted TKIs has been compromised by the emergence of adaptive and acquired resistance through multiple distinct mechanisms (62). These limitations warrant the development of novel, targeted agents. Given the fewer numbers and different catalytic mechanisms of DUBs (63), we believe that they will become a new class of potential drug targets. In this study, we observed that thiolutin, an inhibitor of BRCC36 (43), reduced the level of p-STAT5, impaired cell proliferation, and promoted apoptosis in ITD cells such as MV4-11 cells. Furthermore, these effects of thiolutin exhibited mutual synergies with quizartinib, a TKI used for AML. Recent research has suggested that thiolutin holds promise for the clinical therapy of esophageal squamous cell carcinoma (64), further indicating that BRCC36 could be a potential therapeutic target for treating AML with FLT3-ITD.

5. References

1.Lao, L., Bourdeau, I., Gagliardi, L., He, X., Shi, W., Hao, B., et al. (2022) ARMC5 is part of an RPB1-specific ubiquitin ligase implicated in adrenal hyperplasia. *Nucleic Acids Res* **50**, 6343-6367

2.Korac, J., Schaeffer, V., Kovacevic, I., Clement, A. M., Jungblut, B., Behl, C., et al. (2013) Ubiquitin-independent function of optineurin in autophagic clearance of protein aggregates. *J Cell Sci* **126**, 580-592

3.Clague, M. J., and Urbe, S. (2006) Endocytosis: the DUB version. *Trends Cell Biol* **16**, 551-559

4.Swatek, K. N., and Komander, D. (2016) Ubiquitin modifications. *Cell Res* **26**, 399-422

5.Zong, Z., Zhang, Z., Wu, L., Zhang, L., and Zhou, F. (2021) The Functional Deubiquitinating Enzymes in Control of Innate Antiviral Immunity. *Adv Sci (Weinh)* **8**, 2002484

6.Yau, R., and Rape, M. (2016) The increasing complexity of the ubiquitin code. *Nat Cell Biol* **18**, 579-586

7.Ohtake, F., Saeki, Y., Ishido, S., Kanno, J., and Tanaka, K. (2016) The K48-K63 Branched Ubiquitin Chain Regulates NF-kappaB Signaling. *Mol Cell* **64**, 251-266

8.Li, W., and Ye, Y. (2008) Polyubiquitin chains: functions, structures, and mechanisms. *Cell Mol Life Sci* **65**, 2397-2406

9.Duncan, L. M., Piper, S., Dodd, R. B., Saville, M. K., Sanderson, C. M., Luzio, J. P., et al. (2006) Lysine-63-linked ubiquitination is required for endolysosomal degradation of class I molecules. *EMBO J* **25**, 1635-1645

10.Zeqiraj, E., Tian, L., Piggott, C. A., Pillon, M. C., Duffy, N. M., Ceccarelli, D. F., et al. (2015) Higher-Order Assembly of BRCC36-KIAA0157 Is Required for DUB Activity and Biological Function. *Mol Cell* **59**, 970-983

11.Rabl, J., Bunker, R. D., Schenk, A. D., Cavadini, S., Gill, M. E., Abdulrahman, W., et al. (2019) Structural Basis of BRCC36 Function in DNA Repair and Immune Regulation. *Mol Cell* **75**, 483-497.e489

12.Rabl, J. (2020) BRCA1-A and BRISC: Multifunctional Molecular Machines for Ubiquitin Signaling. *Biomolecules* **10**

13.Maifrede, S., Nieborowska-Skorska, M., Sullivan-Reed, K., Dasgupta, Y., Podszywalow-Bartnicka, P., Le, B. V., et al. (2018) Tyrosine kinase inhibitor-induced defects in DNA repair sensitize FLT3(ITD)-positive leukemia cells to PARP1 inhibitors. *Blood* **132**, 67-77

14.Kazi, J. U., and Ronnstrand, L. (2019) FMS-like Tyrosine Kinase 3/FLT3: From Basic Science to Clinical Implications. *Physiol Rev* **99**, 1433-1466

15.Kikushige, Y., Yoshimoto, G., Miyamoto, T., Iino, T., Mori, Y., Iwasaki, H., et al. (2008) Human Flt3 is expressed at the hematopoietic stem cell and the granulocyte/macrophage progenitor stages to maintain cell survival. *J Immunol* **180**, 7358-7367

16.Kottaridis, P. D., Gale, R. E., and Linch, D. C. (2003) Flt3 mutations and leukaemia.

Br J Haematol **122**, 523-538
17.Levis, M., Brown, P., Smith, B. D., Stine, A., Pham, R., Stone, R., et al. (2006) Plasma inhibitory activity (PIA): a pharmacodynamic assay reveals insights into the basis for cytotoxic response to FLT3 inhibitors. *Blood* **108**, 3477-3483
18.Janke, H., Pastore, F., Schumacher, D., Herold, T., Hopfner, K. P., Schneider, S., et al. (2014) Activating FLT3 mutants show distinct gain-of-function phenotypes in vitro and a characteristic signaling pathway profile associated with prognosis in acute myeloid leukemia. *PLoS One* **9**, e89560
19.Kayser, S., Schlenk, R. F., Londono, M. C., Breitenbuecher, F., Wittke, K., Du, J., et al. (2009) Insertion of FLT3 internal tandem duplication in the tyrosine kinase domain-1 is associated with resistance to chemotherapy and inferior outcome. *Blood* **114**, 2386-2392
20.Gale, R. E., Green, C., Allen, C., Mead, A. J., Burnett, A. K., Hills, R. K., et al. (2008) The impact of FLT3 internal tandem duplication mutant level, number, size, and interaction with NPM1 mutations in a large cohort of young adult patients with acute myeloid leukemia. *Blood* **111**, 2776-2784
21.Burchert, A. (2021) Maintenance therapy for FLT3-ITD-mutated acute myeloid leukemia. *Haematologica* **106**, 664-670
22.Leischner, H., Albers, C., Grundler, R., Razumovskaya, E., Spiekermann, K., Bohlander, S., et al. (2012) SRC is a signaling mediator in FLT3-ITD- but not in FLT3-TKD-positive AML. *Blood* **119**, 4026-4033
23.Rudorf, A., Müller, T. A., Klingeberg, C., Kreutmair, S., Poggio, T., Gorantla, S. P., et al. (2019) NPM1c alters FLT3-D835Y localization and signaling in acute myeloid leukemia. *Blood* **134**, 383-388
24.Choudhary, C., Schwable, J., Brandts, C., Tickenbrock, L., Sargin, B., Kindler, T., et al. (2005) AML-associated Flt3 kinase domain mutations show signal transduction differences compared with Flt3 ITD mutations. *Blood* **106**, 265-273
25.Grundler, R., Miething, C., Thiede, C., Peschel, C., and Duyster, J. (2005) FLT3-ITD and tyrosine kinase domain mutants induce 2 distinct phenotypes in a murine bone marrow transplantation model. *Blood* **105**, 4792-4799
26.Cho, K. F., Branon, T. C., Udeshi, N. D., Myers, S. A., Carr, S. A., and Ting, A. Y. (2020) Proximity labeling in mammalian cells with TurboID and split-TurboID. *Nat Protoc* **15**, 3971-3999
27.Duan, C., Fukuda, T., Isaji, T., Qi, F., Yang, J., Wang, Y., et al. (2020) Deficiency of core fucosylation activates cellular signaling dependent on FLT3 expression in a Ba/F3 cell system. *FASEB J* **34**, 3239-3252
28.Takahashi, S., and Shirahama, K. (2016) Internal tandem duplication and tyrosine kinase domain mutations in FLT3 alter the response to daunorubicin in Ba/F3 cells. *Biomed Rep* **4**, 83-86
29.Branon, T. C., Bosch, J. A., Sanchez, A. D., Udeshi, N. D., Svinkina, T., Carr, S. A., et al. (2018) Efficient proximity labeling in living cells and organisms with TurboID. *Nat Biotechnol* **36**, 880-887
30.Song, W., Isaji, T., Nakano, M., Liang, C., Fukuda, T., and Gu, J. (2022) O-GlcNAcylation regulates beta1,4-GlcNAc-branched N-glycan biosynthesis via the

OGT/SLC35A3/GnT-IV axis. *FASEB J* **36**, e22149
31.Lim, K. L., Chew, K. C., Tan, J. M., Wang, C., Chung, K. K., Zhang, Y., et al. (2005) Parkin mediates nonclassical, proteasomal-independent ubiquitination of synphilin-1: implications for Lewy body formation. *J Neurosci* **25**, 2002-2009
32.Zhang, G., Isaji, T., Xu, Z., Lu, X., Fukuda, T., and Gu, J. (2019) N-acetylglucosaminyltransferase-I as a novel regulator of epithelial-mesenchymal transition. *FASEB J* **33**, 2823-2835
33.Motani, K., and Kosako, H. (2020) BioID screening of biotinylation sites using the avidin-like protein Tamavidin 2-REV identifies global interactors of stimulator of interferon genes (STING). *J Biol Chem* **295**, 11174-11183
34.Rossio, V., Paulo, J. A., Chick, J., Brasher, B., Gygi, S. P., and King, R. W. (2021) Proteomics of broad deubiquitylase inhibition unmasks redundant enzyme function to reveal substrates and assess enzyme specificity. *Cell Chem Biol* **28**, 487-502.e485
35.Izumi, K., Yamashina, S., Fujimura, T., Watanabe, S., and Ikejima, K. (2022) Autophagic dysfunction in the liver enhances the expression of insoluble nuclear proteins 14-3-3ζ and importin α4. *Life Sci* **298**, 120491
36.Yao, T., Fujimura, T., Murayama, K., Okumura, K., and Seko, Y. (2022) Oxidative stress-responsive apoptosis inducing protein (ORAIP) plays a critical role in doxorubicin-induced apoptosis in rat cardiac myocytes. *Int J Cardiol* **348**, 119-124
37.Barbati, C., Vomero, M., Colasanti, T., Diociaiuti, M., Ceccarelli, F., Ferrigno, S., et al. (2018) TNFα expressed on the surface of microparticles modulates endothelial cell fate in rheumatoid arthritis. *Arthritis Res Ther* **20**, 273
38.Schmidt-Arras, D. E., Böhmer, A., Markova, B., Choudhary, C., Serve, H., and Böhmer, F. D. (2005) Tyrosine phosphorylation regulates maturation of receptor tyrosine kinases. *Mol Cell Biol* **25**, 3690-3703
39.Choudhary, C., Olsen, J. V., Brandts, C., Cox, J., Reddy, P. N., Böhmer, F. D., et al. (2009) Mislocalized activation of oncogenic RTKs switches downstream signaling outcomes. *Mol Cell* **36**, 326-339
40.Reiter, K., Polzer, H., Krupka, C., Maiser, A., Vick, B., Rothenberg-Thurley, M., et al. (2018) Tyrosine kinase inhibition increases the cell surface localization of FLT3-ITD and enhances FLT3-directed immunotherapy of acute myeloid leukemia. *Leukemia* **32**, 313-322
41.Alvarez, C., and Sztul, E. S. (1999) Brefeldin A (BFA) disrupts the organization of the microtubule and the actin cytoskeletons. *Eur J Cell Biol* **78**, 1-14
42.Cooper, E. M., Cutcliffe, C., Kristiansen, T. Z., Pandey, A., Pickart, C. M., and Cohen, R. E. (2009) K63-specific deubiquitination by two JAMM/MPN+ complexes: BRISC-associated Brcc36 and proteasomal Poh1. *Embo j* **28**, 621-631
43.Lauinger, L., Li, J., Shostak, A., Cemel, I. A., Ha, N., Zhang, Y., et al. (2017) Thiolutin is a zinc chelator that inhibits the Rpn11 and other JAMM metalloproteases. *Nat Chem Biol* **13**, 709-714
44.Kazi, J. U., Sun, J., Phung, B., Zadjali, F., Flores-Morales, A., and Rönnstrand, L. (2012) Suppressor of cytokine signaling 6 (SOCS6) negatively regulates Flt3 signal transduction through direct binding to phosphorylated tyrosines 591 and 919 of Flt3. *J Biol Chem* **287**, 36509-36517

45.Zarrinkar, P. P., Gunawardane, R. N., Cramer, M. D., Gardner, M. F., Brigham, D., Belli, B., et al. (2009) AC220 is a uniquely potent and selective inhibitor of FLT3 for the treatment of acute myeloid leukemia (AML). *Blood* **114**, 2984-2992
46.Kellner, F., Keil, A., Schindler, K., Tschongov, T., Hunninger, K., Loercher, H., et al. (2020) Wild-type FLT3 and FLT3 ITD exhibit similar ligand-induced internalization characteristics. *J Cell Mol Med* **24**, 4668-4676
47.Oshikawa, G., Nagao, T., Wu, N., Kurosu, T., and Miura, O. (2011) c-Cbl and Cbl-b ligases mediate 17-allylaminodemethoxygeldanamycin-induced degradation of autophosphorylated Flt3 kinase with internal tandem duplication through the ubiquitin proteasome pathway. *J Biol Chem* **286**, 30263-30273
48.Grafone, T., Palmisano, M., Nicci, C., and Storti, S. (2012) An overview on the role of FLT3-tyrosine kinase receptor in acute myeloid leukemia: biology and treatment. *Oncol Rev* **6**, e8
49.Choudhary, C., Olsen, J. V., Brandts, C., Cox, J., Reddy, P. N., Bohmer, F. D., et al. (2009) Mislocalized activation of oncogenic RTKs switches downstream signaling outcomes. *Mol Cell* **36**, 326-339
50.Schmidt-Arras, D., Böhmer, S. A., Koch, S., Müller, J. P., Blei, L., Cornils, H., et al. (2009) Anchoring of FLT3 in the endoplasmic reticulum alters signaling quality. *Blood* **113**, 3568-3576
51.Kelly, L. M., Liu, Q., Kutok, J. L., Williams, I. R., Boulton, C. L., and Gilliland, D. G. (2002) FLT3 internal tandem duplication mutations associated with human acute myeloid leukemias induce myeloproliferative disease in a murine bone marrow transplant model. *Blood* **99**, 310-318
52.Maspero, E., Valentini, E., Mari, S., Cecatiello, V., Soffientini, P., Pasqualato, S., et al. (2013) Structure of a ubiquitin-loaded HECT ligase reveals the molecular basis for catalytic priming. *Nat Struct Mol Biol* **20**, 696-701
53.Akiyama, H., Umezawa, Y., Ishida, S., Okada, K., Nogami, A., and Miura, O. (2019) Inhibition of USP9X induces apoptosis in FLT3-ITD-positive AML cells cooperatively by inhibiting the mutant kinase through aggresomal translocation and inducing oxidative stress. *Cancer Lett* **453**, 84-94
54.Weisberg, E. L., Schauer, N. J., Yang, J., Lamberto, I., Doherty, L., Bhatt, S., et al. (2017) Inhibition of USP10 induces degradation of oncogenic FLT3. *Nat Chem Biol* **13**, 1207-1215
55.Zhao, L., Zhao, J., Zhong, K., Tong, A., and Jia, D. (2022) Targeted protein degradation: mechanisms, strategies and application. *Signal Transduct Target Ther* **7**, 113
56.Donaghy, R., Han, X., Rozenova, K., Lv, K., Jiang, Q., Doepner, M., et al. (2019) The BRISC deubiquitinating enzyme complex limits hematopoietic stem cell expansion by regulating JAK2 K63-ubiquitination. *Blood* **133**, 1560-1571
57.Thiede, C., Steudel, C., Mohr, B., Schaich, M., Schäkel, U., Platzbecker, U., et al. (2002) Analysis of FLT3-activating mutations in 979 patients with acute myelogenous leukemia: association with FAB subtypes and identification of subgroups with poor prognosis. *Blood* **99**, 4326-4335
58.Beitinjaneh, A., Jang, S., Roukoz, H., and Majhail, N. S. (2010) Prognostic

significance of FLT3 internal tandem duplication and tyrosine kinase domain mutations in acute promyelocytic leukemia: a systematic review. *Leuk Res* **34**, 831-836
59.Oyarzo, M. P., Lin, P., Glassman, A., Bueso-Ramos, C. E., Luthra, R., and Medeiros, L. J. (2004) Acute myeloid leukemia with t(6;9)(p23;q34) is associated with dysplasia and a high frequency of flt3 gene mutations. *Am J Clin Pathol* **122**, 348-358
60.Steudel, C., Wermke, M., Schaich, M., Schäkel, U., Illmer, T., Ehninger, G., et al. (2003) Comparative analysis of MLL partial tandem duplication and FLT3 internal tandem duplication mutations in 956 adult patients with acute myeloid leukemia. *Genes Chromosomes Cancer* **37**, 237-251
61.Jiang, K., Li, X., Wang, C., Hu, X., Wang, P., Tong, L., et al. (2022) Dual inhibition of CHK1/FLT3 enhances cytotoxicity and overcomes adaptive and acquired resistance in FLT3-ITD acute myeloid leukemia. *Leukemia*
62.Williams, A. B., Li, L., Nguyen, B., Brown, P., Levis, M., and Small, D. (2012) Fluvastatin inhibits FLT3 glycosylation in human and murine cells and prolongs survival of mice with FLT3/ITD leukemia. *Blood* **120**, 3069-3079
63.Birol, M., and Echalier, A. (2014) Structure and function of MPN (Mpr1/Pad1 N-terminal) domain-containing proteins. *Curr Protein Pept Sci* **15**, 504-517
64.Jing, C., Li, X., Zhou, M., Zhang, S., Lai, Q., Liu, D., et al. (2021) The PSMD14 inhibitor Thiolutin as a novel therapeutic approach for esophageal squamous cell carcinoma through facilitating SNAIL degradation. *Theranostics* **11**, 5847-5862

6. Abbreviations

AML, acute myeloid leukemia; BFA, brefeldin A; BRCC36, BRCA1/BRCA2-containing complex subunit 36; CHX, cycloheximide; DUB, deubiquitinase; FLT3, Fms-like tyrosine kinase-3; GnT-I, N-acetylglucosaminyltransferase-I; ITD, internal-tandem duplication domain; NEDD4, neural precursor cell-expressed developmentally downregulated protein 4; STAT5, signal transducers and activators of transcription 5; Thl, thiolutin; TKD, tyrosine kinase domain; TKI, tyrosine kinase domain; Ub, ubiquitin.

7. Acknowledgments

I would like to express my sincere gratitude to the individuals who have supported and assisted me throughout the completion of this graduation thesis. The journey has been challenging, but it has also been filled with opportunities for learning and growth.

Foremost, I express my sincere gratitude to President Motoaki Takayanagi for granting me the opportunity to pursue my studies at Tohoku Medical and Pharmaceutical University.

I extend my deepest appreciation to my supervisor, Professor Jianguo Gu. Thank you for your guidance and insightful mentorship throughout the entire research process. Your expertise, patience, and motivation have been instrumental in driving me to complete this thesis.

I would also like to thank Dr. Tomoya Isaji, Dr. Tomohiko Fukuda and Professor Shinichiro Takahashi for their valuable feedback and suggestions on my thesis. With your assistance, my research has become more comprehensive and profound. Thanks for the technique helps from Professor Tsutomu Fujimura and Dr. Sachiko Komatsu. I also extend my gratitude to Ms. Yan Hao and my friends for their help and shared experiences.

Finally, I would like to acknowledge my family and all those people who have made efforts and contributions to completion of this dissertation.